Research Article

Green preparation of chlorine-doped graphene and its application in electrochemical sensor for chloramphenicol detection

Kai-Ping Wang[1] · Yi-Chi Zhang[1] · Xuan Zhang[1,2] · Li Shen[1]

Abstract
A green but efficient synthesis approach for chlorine-doped reduced graphene oxide (Cl-RGO) was developed. The chlorine-doping and reduction was achieved in one-step by refluxing graphene oxide solution in concentrated hydrochloric acid (8 M, 120 °C) under N_2 atmosphere. X-ray photoelectron spectroscopy analysis revealed that the Cl content was 1.01 at.% in the Cl-RGO. Electrochemical measurements indicated that the Cl-RGO modified glass carbon electrode showed enhanced electrochemical conductivity and electrocatalytic activity for the veterinary drug chloramphenicol (CAP) detection. Thus a highly selective electrochemical sensor for CAP was constructed based on Cl-RGO, and a linear relationship between current intensity and CAP concentration (2–35 μM) was obtained with a detection limit of 1 μM (S/N = 3). The sensor showed excellent reproducibility, storage stability and was successfully used for CAP detection in milk, calf plasma, water and pharmaceutical samples.

Keywords Chlorine-doped graphene · Electrochemical sensor · Chloramphenicol · Green synthesis

1 Introduction

Chloramphenicol (CAP) is a broad-spectrum antibacterial veterinary drug and has been extensively used for the treatment of infectious diseases in animals. However, it has been recognized that the CAP may cause many chronic diseases such as bone marrow depression, aplastic anemia and cardiovascular collapse [1–3]. As a consequence, the use of CAP in animals-derived food has been globally banned to control the food safety. The increasing concerns about food safety urged the development of rapid, selective and sensitive analytical methods to monitor CAP residue in food and water samples.

Nowadays, various conventional analytical methods, such as liquid chromatography-mass spectroscopy (LC–MS) [4], gas chromatography-mass spectroscopy (GC–MS) [5], capillary electrophoresis (CE) [6], and chemiluminescent immunoassay [7], have been put forward for CAP residue detection. Nevertheless, complicated pretreatment processes, expensive instruments and professional operator requirements make these methods not suitable to routine and rapid analysis of samples. Alternatively, electrochemical method has the advantages of rapid analysis, cheap equipment and simple operation [8, 9]. Thus many electrochemical sensors for CAP detection based on various electrode materials have been developed [10–17]. Among these electrode materials, various nanomaterials such as carbon and metal nanoparticles, have been employed for antibiotics drug residues detection in animal-derived food and water samples [18–21]. As a typical carbon nanomaterial, graphene has drawn increasing interest as electrode materials because of its

Electronic supplementary material The online version of this article (https://doi.org/10.1007/s42452-019-0174-4) contains supplementary material, which is available to authorized users.

✉ Xuan Zhang, xzhang@dhu.edu.cn | [1]Key Laboratory of Science and Technology of Eco-Textiles, Ministry of Education, College of Chemistry, Chemical Engineering and Biotechnology, Donghua University, Shanghai 201620, China. [2]Key Laboratory of Polar Materials and Devices, Ministry of Education, East China Normal University, Shanghai 200241, China.

SN Applied Sciences (2019) 1:157 | https://doi.org/10.1007/s42452-019-0174-4

Received: 4 December 2018 / Accepted: 8 January 2019 / Published online: 10 January 2019

excellent electrical conductivity, high surface area and mechanical strength [22]. Recently, graphene-based electrochemical sensors for CAP have been developed, for example, titanium nitride–reduced graphene oxide nanohybrids [13], gold nanoparticles/nitrogen-doped graphene [23], silver nanoparticles/graphene composite [24, 25]. Most of these reported graphene-based electrode materials require complicated preparation processes and the electrochemical sensing performances should be further improved.

As well-known, heteroatom-doping was an effective approach to tailor the electrochemical properties of graphene materials [26–28]. In this regard, nitrogen-, sulfur-, phosphorus- and boron-doped graphene materials have been facilely derived from chemical reduction of graphene oxide (GO) and used as new electrode materials [28–30]. The preparation of heteroatom-doped graphene usually needs harsh experimental condition and toxic chemical regent. In this work, a green and efficient synthesis approach for chlorine-doped reduced graphene oxide (Cl-RGO) was developed. The chlorine-doping and reduction was achieved in one-step by refluxing GO solution in concentrated hydrochloric (HCl) acid under N_2 atmosphere. The Cl-RGO was further used as a novel electrode material to construct electrochemical sensor for veterinary drug CAP detection in milk, calf plasma, water and pharmaceutical samples.

2 Experimental

2.1 Materials

All common chemicals were obtained from Sinopharm Chemical Reagent Corp. (Shanghai, China) at analytical grade. Graphite powder (99.85%) was purchased from XFNANO (Nanjing, China). CAP was supplied by Hefei Bomei Biotechnology Co. Ltd. (China). Phosphate buffer solutions (PBS, 0.1 M) were prepared by mixing K_2HPO_4 and KH_2PO_4 and used for CAP stock solution (3 mM) preparation and electrochemical measurements.

2.2 Preparation of Cl-RGO

GO was firstly produced from graphite powder according to the previously reported procedures [31, 32]. Then the GO (20 mg) was dispersed in water (13 mL) and concentrated hydrochloric acid (27 mL) under ultrasonication for 30 min. The GO solution was transferred into a round bottom flask and heated in oil bath at 120 °C for 6 h under nitrogen atmosphere. After cooling to room temperature, the Cl-RGO was collected by centrifugation, thoroughly washing with water until neutral pH reached, and finally dried in vacuum oven at 45 °C for 12 h.

2.3 Characterization apparatus

The morphology Cl-RGO was characterized by scanning electron microscopy (SEM, Hitachi S-4800, Japan) and transmission electron microscopy (TEM, JEOL JEM-2100F, Japan). X-ray photoelectron spectroscopy (XPS) was recorded on PHI 5400 (USA).

2.4 Electrochemical measurements

The electrochemical measurements were performed as previously described procedures [33]. In brief, cyclic voltammetry (CV) and differential pulse voltammetry (DPV) measurements were performed on Chenhua CHI-660D electrochemical workstation (Shanghai, China) with a standard three-electrode system. Pre-polished glassy carbon electrode (GCE) was coated by Cl-RGO suspension and used as the working electrode (Cl-RGO/GCE), while Pt wire and saturated calomel electrode (SCE) were employed as counter as well as reference electrodes, respectively. The CV measurements were carried out at a potential range between − 0.2 and 0.6 V (vs. SCE) for $[Fe(CN)_6]^{3-/4-}$ or − 0.8 to 0.4 V (vs. SCE) for CAP with the scan rate of 50 mV s^{-1}. The DPV measurements was finished at a potential window between − 0.4 and − 0.8 V (vs. SCE), with step potential of 4 mV, amplitude of 50 mV, pulse width of 0.2 s and pulse period of 0.5 s, respectively.

3 Results and discussion

3.1 Optimization of preparation conditions for Cl-RGO

The optimal reduction conditions for preparation of Cl-RGO were firstly investigated by CV measurement, where $K_3[Fe(CN)_6]$ was employed as redox probe and the graphene materials obtained at different reaction conditions was used to modify GCE, respectively. As shown in Fig. 1a–c, the peak current intensity was strongly dependent on the concentration of HCl acid, reaction temperature and time, and the optimal conditions are respectively 8 M, 120 °C and 6 h. Then the Cl-RGO material obtained at the above optimal conditions was coated on GCE to construct electrochemical sensor (Cl-RGO/GCE). Subsequently, the electroactive surface area (EASA) and electrical conductivity property of Cl-RGO/GCE were comparatively studied with those of the bare GCE. As shown in Fig. 1d, a pair of well-defined CV redox peaks of $K_3[Fe(CN)_6]$ appeared on both electrodes, but the higher peak current was observed

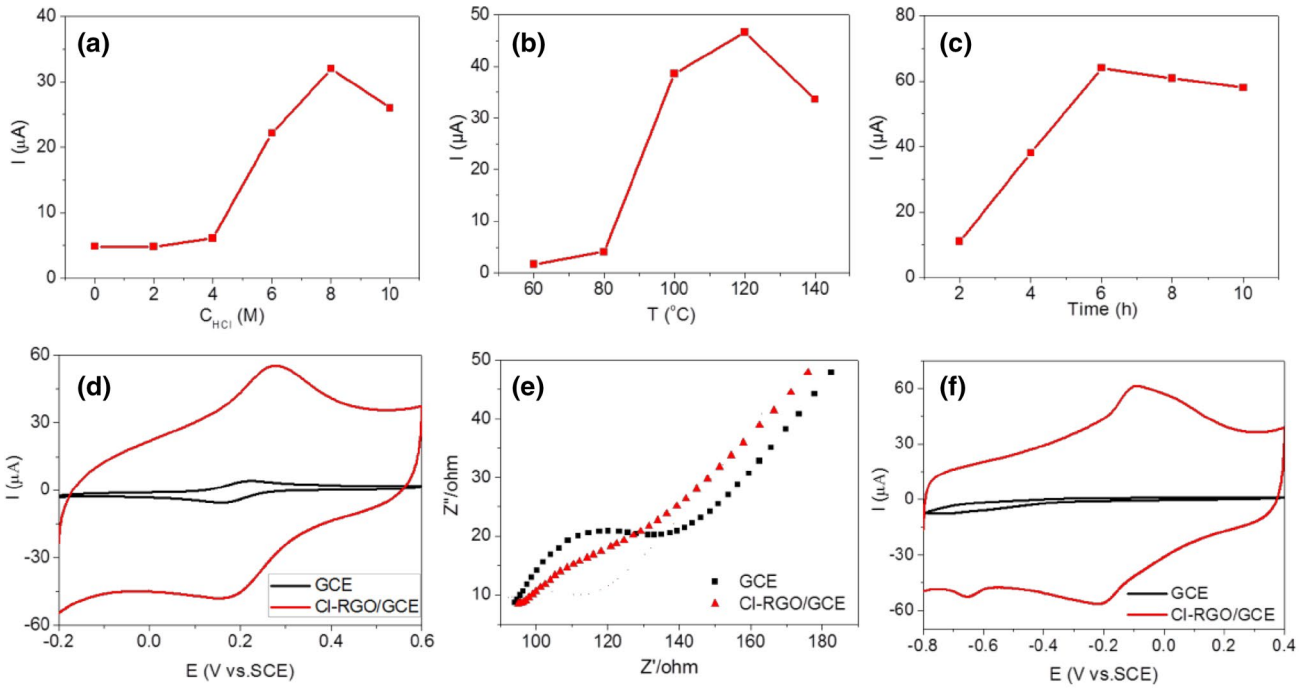

Fig. 1 The relationships between the forward peak current intensity of 0.5 M $K_3[Fe(CN)_6]$ on Cl-RGO/GCE at 0.275 V and concentration of HCl acid (**a**), reduction temperature (**b**) and reduction time (**c**). CV (**d**) and EIS (**e**) curves of 0.5 mM $K_3[Fe(CN)_6]$ in 0.1 M KCl measured on Cl-RGO/GCE and bare GCE, respectively. CV curves of 50 μM CAP in 0.1 M PBS solution (pH 7.4) measured on Cl-RGO/GCE and bare GCE, respectively (**f**)

on the Cl-RGO electrode. The enhancement of current intensity could be related to an enlarged effective EASA. According to the Randles–Sevcik equation [34], the EASA value was estimated to be 0.42 and 0.07 cm^2 for Cl-RGO/GCE and bare GCE respectively, confirming that the utilization of Cl-RGO as novel electrode material could effectively increase EASA by sixfolds over bare GCE. To evaluate the electrical conductivity, electrochemical impedance spectroscopy (EIS) analysis was performed in 0.1 M KCl solution containing 0.5 mM $K_3[Fe(CN)_6]$. Figure 1e showed the EIS respectively obtained on Cl-RGO/GCE and bare GCE, and the smaller semicircle domains observed on Cl-RGO/GCE suggested its lower electron transfer resistance [35]. Both the larger EASA and higher electrical conductivity make the Cl-RGO/GCE promising platform for electrochemical sensor construction. As a proof of concept, CV measurements were performed in 0.1 M PBS solution containing 50 μM CAP. It can be seen that the higher current intensity was obtained on Cl-RGO/GCE, where one forward anodic peak appeared at − 0.097 V and two cathodic peaks appeared at − 0.21 and − 0.65 V respectively (Fig. 1f). The cathodic peak at − 0.65 V was due to the irreversible reduction of the nitro group, whereas the other two peaks were attributed to the redox of the hydroxylamine group [23]. This indicates that Cl-RGO/GCE could be used as a promising electrochemical sensor for CAP detection.

3.2 Characterization of Cl-RGO

The reduction extent of GO in Cl-RGO was investigated by XPS analysis. As shown in the survey XPS spectrum (Fig. 2a), three peaks were observed around 532, 285 and 200 eV those were ascribed to O1s, C1s and Cl2p, respectively. It was found that the C/O ratio was improved to approximately 5:1 of Cl-RGO from 2:1 of GO, indicating an efficient reduction of GO by HCl acid [36]. The high-resolution C1s XPS spectrum of Cl-RGO (Fig. 2b) exhibited three components centered at 284.6, 286.8, 288.5 eV, corresponding to the C–C/C=C in alkyl and sp^2 bonded carbon network, the C–Cl and C-O in hydroxyl and epoxy groups, and the C=O in carbonyl and ketone, respectively. Notably, the C1s peak intensities related to oxygen functional groups in Cl-RGO were much weaker than those in GO (Fig. 2d), further confirming the efficient reduction of GO by HCl acid. The high-resolution Cl2p XPS spectrum of Cl-RGO (Fig. 2c) exhibited doublets at 201.8 and 200.3 associated with $2p_{3/2}$ and $2p_{1/2}$ levels due to the spin–orbit coupling, which is a typical indication of organic C–Cl covalent bond formation [37]. Moreover, The Cl content was estimated to be 1.01 atom% by XPS semi-quantitative analysis, which is very close to the value of 0.93 atom% by EDX analysis (Fig. S1). The elemental mapping results indicated that Cl was well-dispersed in graphene materials

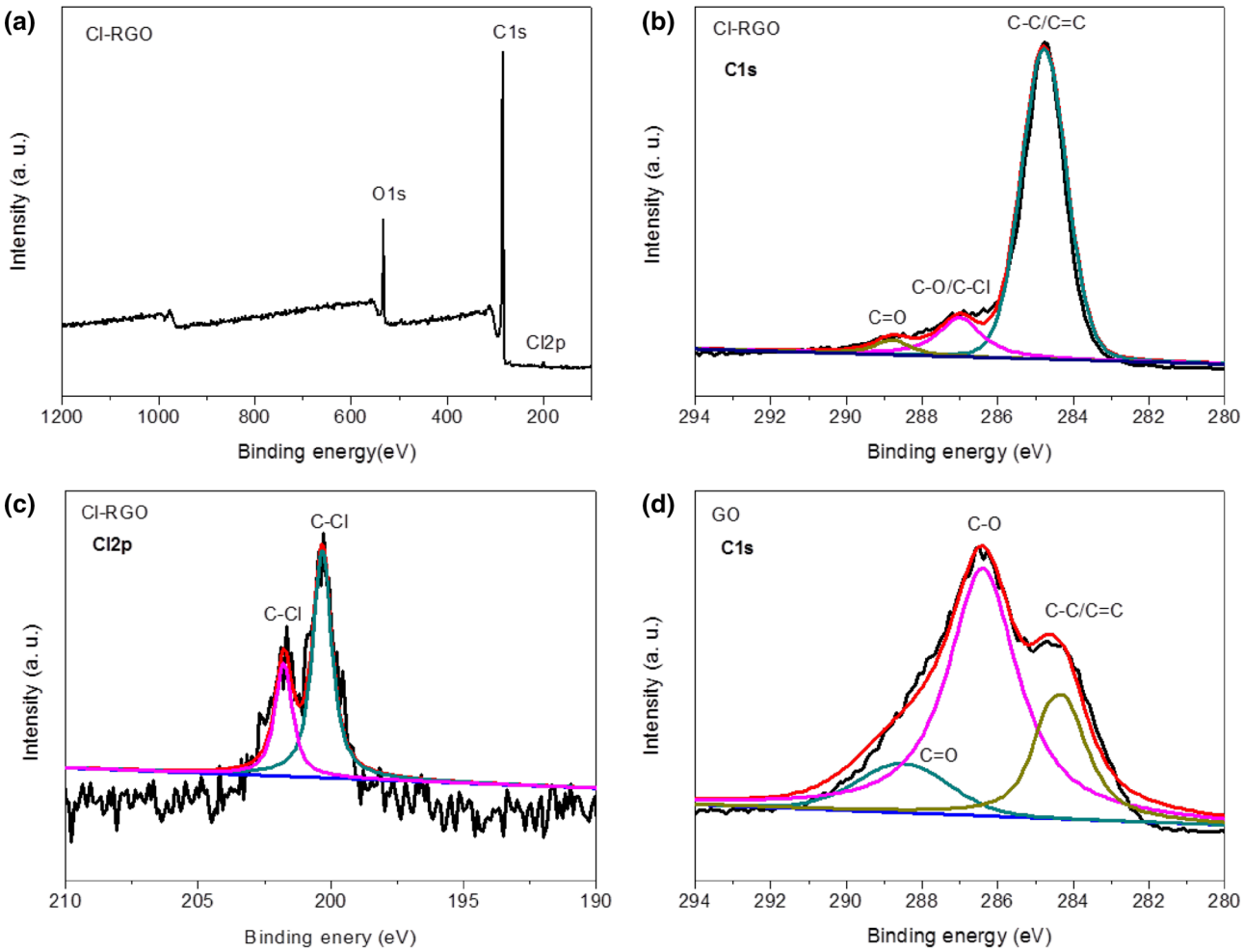

Fig. 2 XPS survey spectrum of Cl-RGO (**a**). High-resolution XPS spectra of the C 1s (**b**) and Cl 2p (**c**) of Cl-RGO as well as C 1s of GO (**d**), respectively

(Fig. S2). These demonstrated that the chlorine-doping and reduction was achieved in one-step and the GO was efficiently converted to be Cl-RGO by HCl acid in this work. The morphology of Cl-RGO was characterized by SEM and TEM and the Cl-RGO sheets clearly showed typically wrinkled ultrathin layer nanostructures with rich ripples (Fig. 3).

3.3 Optimization of determination conditions for CAP

To achieve a high sensitive detection of CAP, the determination conditions, including the pH, utilization amounts and stirring time of Cl-RGO were systematically

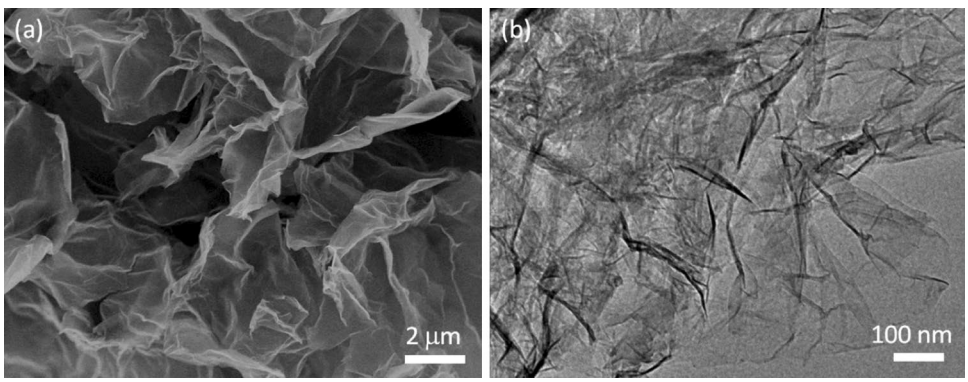

Fig. 3 SEM (**a**) and TEM (**b**) images of Cl-RGO

optimized by DPV measurements. As shown in Fig. 4a, both the peak potentials and currents strongly depend on pH values, demonstrating that the proton took part in the electrochemical reaction process. With changing pH from 4 to 9, while the peak potentials monotonically shifted to negative window, the peak current increased firstly and decreased again and the maximum intensity obtained at pH 7.4 (Fig. 4a, b). The PBS buffer solution with physiological pH 7.4 was therefore chosen as optimal pH in this work. Figure 4e showed the DPV curves of CAP on GCE modified with various amounts of Cl-RGO. Obviously, the current intensity

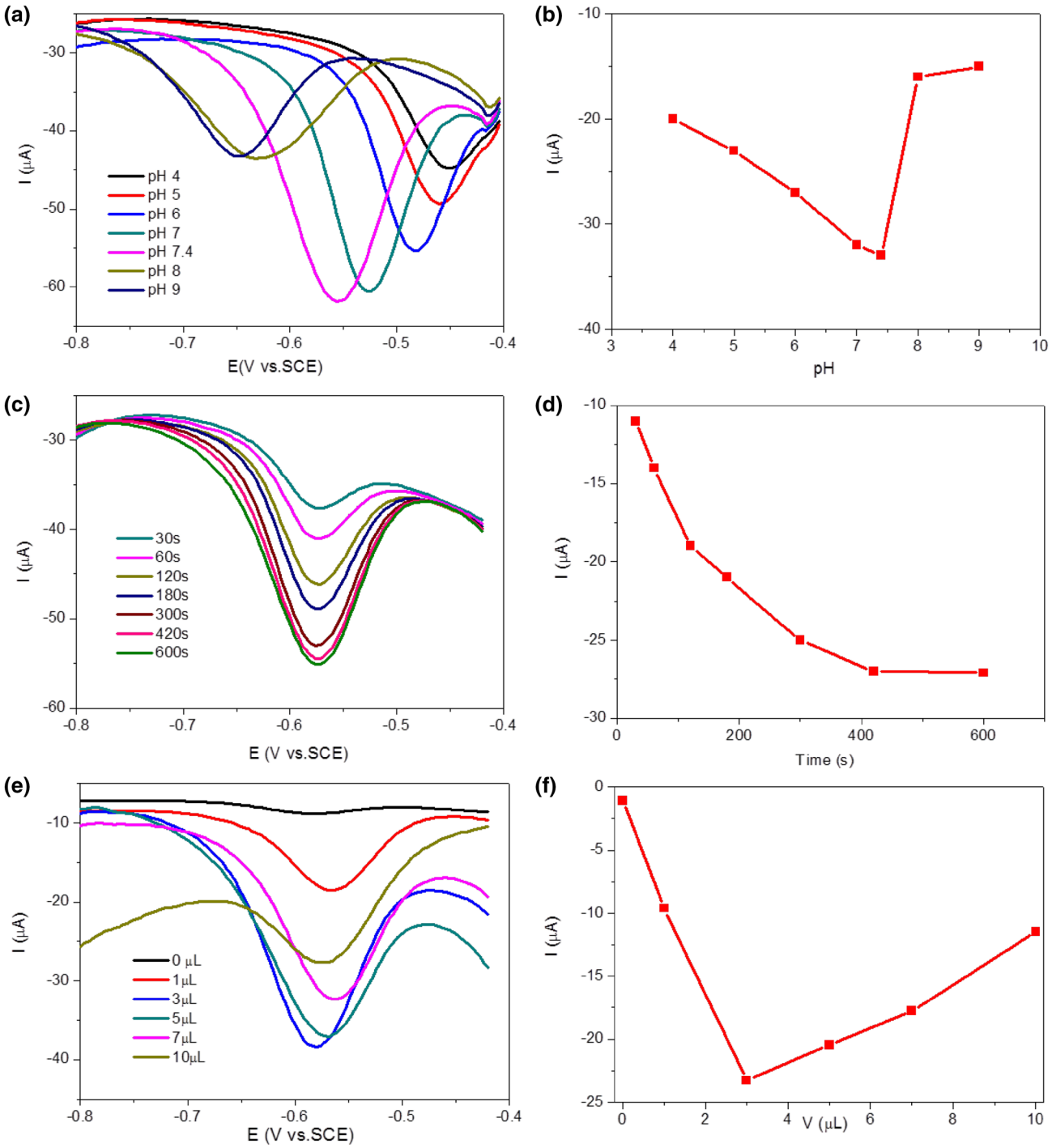

Fig. 4 DPV curves of CAP (50 μM) on Cl-RGO/GCE at various pH (**a**), diffusion time (**b**), usage amounts of Cl-RGO (**c**), and the corresponding relationships between peak current intensity and pH (**a**), diffusion time (**b**), usage amounts of Cl-RGO, respectively

increased with increasing the amounts of Cl-RGO up to 3 µL and decreased after that (Fig. 4f). This demonstrates that the Cl-RGO coating on GCE can effectively enhance the sensitivity due to the improvement of both EASA and electrical conductivity, but excess Cl-RGO could stack to thicker layers that decreased the performance of electrode material. Accordingly, 3 µL of Cl-RGO was used as the optimal utilization amount in this work. The stirring time effect on the peak current of CAP at − 0.65 V was also investigated, which showed a continuously enhancement with increasing stirring time and leveled off up to 420 s (Fig. 4c, d). This suggests that the redox reaction of CAP on the Cl-RGO/GCE could be an adsorption controlled process. Thus all DPV measurements were performed after 420 s stirring of CAP solution in this work. To ascertain the mechanism of CAP redox reaction on the Cl-RGO/GCE, the influence of scan rate (20–100 mV s^{-1}) on the redox peak current was further studied by CV measurements from − 0.8 to 0.4 V (vs. SCE). It can be seen that the current intensities increased with increasing scan rate, and there are good linear relationships between the peak currents and the scan rates, respectively (Fig. 5), confirming the adsorption controlled process nature [34].

3.4 Analytical performances of CAP sensor

Figure 6 displayed the DPV curves of various amounts of CAP on Cl-RGO/GCE electrode under the optimal determination conditions, and the corresponding linear relationship between current intensities and CAP concentrations. It was noticed that the peak current increased with increasing the CAP concentrations over the range of 2–35 µM. The corresponding linear equations is $I = -0.1991C_{CAP} - 0.1109$ ($R^2 = 0.9981$) and the detection limits is 1 µM (S/N = 3) for CAP. Notably, the linear range and detection limit of Cl-RGO/GCE (2–35 µM and 1 µM) are very competitive to those of the previous reported electrochemical CAP sensors, such as 2–80 µM and 0.59 µM [23], 50–1000 µM and 44 µM [38], 10–500 µM and 10 µM [39], respectively.

The selectivity of Cl-RGO/GCE toward CAP was verified in the presence of various potential interfering species.

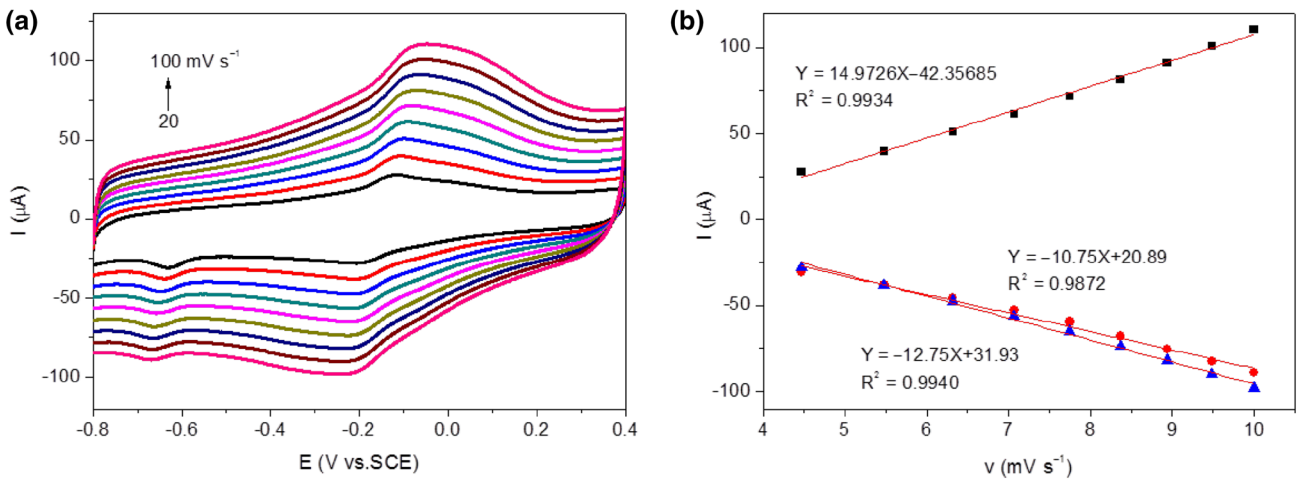

Fig. 5 CV curves of CAP (50 µM) in 0.1 M PBS (pH 7.4) measured on Cl-RGO/GCE at various scan rates (20–100 mV s^{-1}) (**a**), and the corresponding plots of the peak currents versus scan rates (**b**)

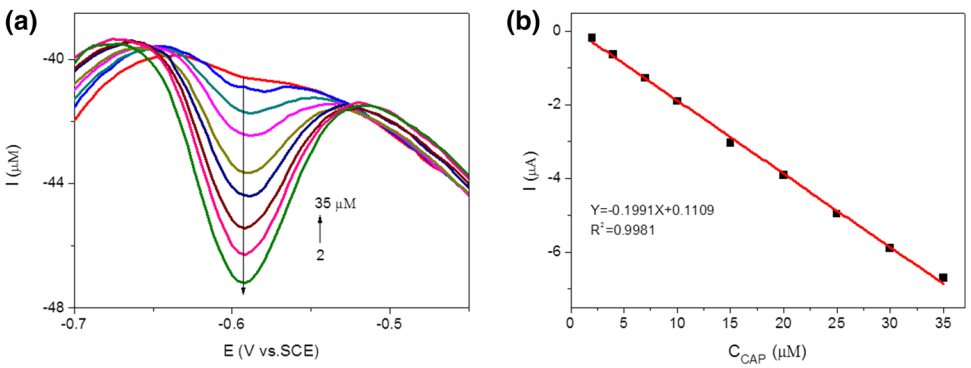

Fig. 6 DPV curves of CAP with various concentrations on Cl-RGO/GCE (**a**) and the corresponding calibration plots between the peak current intensity and CAP concentration (**b**)

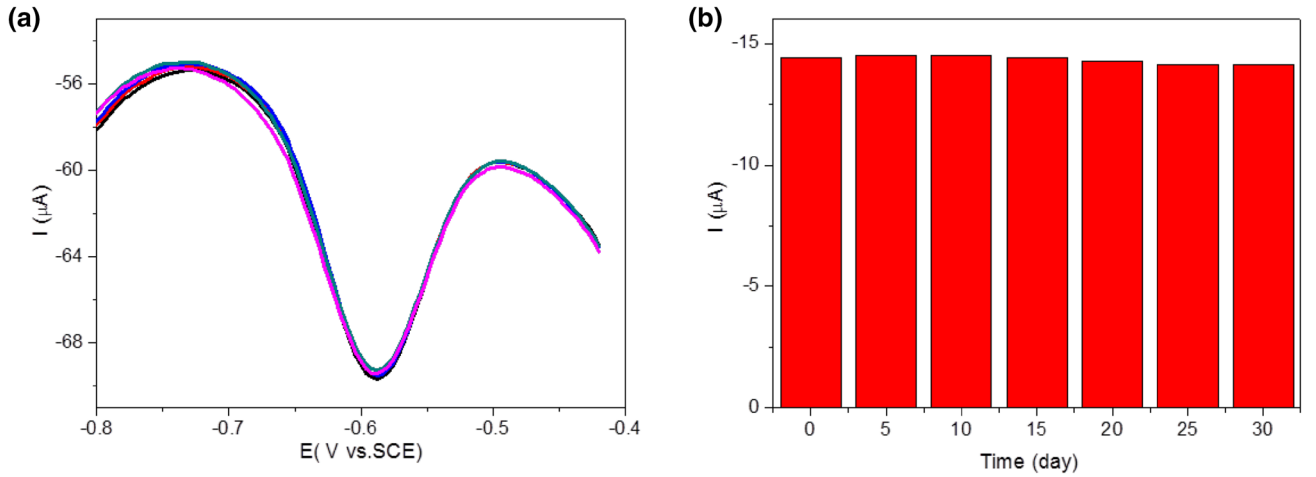

Fig. 7 The DPV curves CAP (50 μM) in 0.1 M PBS (pH 7.4) measured on five different Cl-RGO/GCE electrodes (**a**). Long-term storage stability tests of Cl-RGO/GCE in 0.1 M PBS solution containing 50 μM CAP (**b**)

Table 1 Determination of CAP in real samples

Samples	Added (μM)	Found (μM)	Recovery (%)
Milk	5	5.12 ± 0.3	102.4
	10	10.35 ± 0.5	103.5
Calf plasma	5	5.21 ± 0.2	104.2
	20	20.31 ± 0.9	101.6
Eye drops	/	25.55[a] ± 0.3	/
	5	29.98 ± 0.4	98.1
Tap water	10	10.50 ± 0.1	105.0
	20	19.86 ± 0.2	99.3

[a] Given concentration is 25.79 μM by manufacturer

It was found that only the CAP presented the strong current response, but others interferents showed negligible responses. Moreover, the co-existence of 10 mM glucose as well as common metal ions and anions such as K^+, Na^+, Ca^{2+}, Mg^{2+}, Cu^{2+}, Zn^{2+}, Fe^{2+}, Cl^-, and NO_3^-, 1 mM cysteine, penicillin G, erythromycin, and tetracycline did not affect the detection of 50 μM CAP. Thus the present Cl-RGO/GCE has excellent anti-interference ability and can be used for selective detection of CAP. Additionally, the reproducibility and stability of the electrochemical sensor were critical requirements for antibiotics detection in real samples. Therefore, five Cl-RGO/GCE electrodes were independently fabricated and used for DPV measurements to test the reproducibility, whereas the long-term storage stability was investigated by exposing the same electrode into air for 1 month. As shown in Fig. 7a, the five electrodes exhibited negligible difference on response toward 50 μM CAP and the relative standard deviation (RSD) is as low as 1.5%. It was also noted that the peak current measured every 5 days on the same Cl-RGO/GCE electrode remained almost no change during 30 days storage (Fig. 7b). These results demonstrate that the present sensor has the excellent reproducibility and stability, and could be used for CAP detection in real samples.

3.5 CAP detection in real samples

To demonstrate the practical application potential of the Cl-RGO/GCE sensor for CAP detection, the sensing performance in real samples such as fresh milk, calf plasma, tap water and pharmaceutical chloramphenicol eye drops were investigated by using the standard addition method. All samples were centrifuged at 10,000 rpm for 15 min and directly used for analysis, except the pharmaceutical eye drops samples was diluted 300 times before measurement. Upon addition of certain amounts of CAP, the sample solutions were used for DPV measurements and the results were summarized in Table 1. Notably, the recovery results are 98–105% that is satisfactory. Thus the Cl-RGO/GCE senor is sensitive and selective for a practical CAP detection in food, water and pharmaceutical samples.

4 Conclusions

In summary, chlorine-doped reduced graphene oxide (Cl-RGO) was greenly fabricated and used as novel electrode material for electrochemical sensor. The efficient chlorine-doping (1.01 at.%) and reduction was achieved in one-step by refluxing graphene oxide (GO) solution in concentrated hydrochloric acid under N_2 atmosphere. The electrochemical sensor for veterinary drug chloramphenicol (CAP)

detection was constructed based on Cl-RGO coating on glass carbon electrode (GCE) with a detection limit of 1 μM (S/N = 3). Furthermore, the sensor showed excellent anti-interference ability, reproducibility, stability, and was successfully used for determination of CAP in milk, calf plasma, water and pharmaceutical samples with satisfactory recovery result. The simple and green preparation procedure as well as excellent electrocatalytic ability of Cl-RGO/GCE would be benefit for developing of electrochemical sensor for hazardous antibiotics detection in food safety testing.

Funding This study was funded by Shanghai Municipal Natural Science Foundation (16ZR1401700) and the Open Research Fund of Key Laboratory of Polar Materials and Devices, Ministry of Education.

Compliance with ethical standards

Conflict of interest The authors declare that they have no conflict of interest.

References

1. Gross BJ, Branchflower RV, Burke TR, Lees DE, Pohl LR (1982) Bone marrow toxicity in vitro of chloramphenicol and its metabolites. Toxicol Appl Pharmacol 64:557–565
2. Hanekamp JC, Bast A (2015) Antibiotics exposure and health risks: chloramphenicol. Environ Toxicol Phar 39:213–220
3. Turton JA, Andrews CM, Havard AC, Williams TC (2002) Studies on the haemotoxicity of chloramphenicol succinate in the Dunkin Hartley guinea pig. Int J Exp Pathol 83:225–238
4. Sniegocki T, Posyniak A, Gbylik-Sikorska M, Zmudzki J (2014) Determination of chloramphenicol in milk using a quechers-based on liquid chromatography tandem mass spectrometry method. Anal Lett 47:568–578
5. Azzouz A, Ballesteros E (2015) Multiresidue method for the determination of pharmacologically active substances in egg and honey using a continuous solid-phase extraction system and gas chromatography–mass spectrometry. Food Chem 178:63–69
6. Vera-Candiotia L, Olivieri AC, Goicoechea HC (2010) Development of a novel strategy for preconcentration of antibiotic residues in milk and their quantitation by capillary electrophoresis. Talanta 82:213–221
7. Xu K, Sun Y, Li W, Xu J, Cao B, Jiang Y, Zheng T, Li J, Pan D (2014) Multiplex chemiluminescent immunoassay for screening of mycotoxins using photonic crystal microsphere suspension array. Analyst 139:771–777
8. Pilehvar S, Gielkens K, Trashin SA, Dardenne F, Blust R, De Wael K (2016) (Electro)Sensing of phenicol antibiotics—a review. Criti. Rev. Food Sci. 56:2416–2429
9. Sadeghi AS, Ansari N, Ramezani M, Abnous K, Mohsenzadeh M, Taghdisi SM, Alibolandi M (2018) Optical and electrochemical aptasensors for the detection of amphenicols. Biosens Bioelectron 118:137–152
10. Zhang X, Zhang YC, Zhang JW (2016) A highly selective electrochemical sensor for chloramphenicol based on three-dimensional reduced graphene oxide architectures. Talanta 161:567–573
11. Zhang W, Zhang Z, Li Y, Chen J, Li X, Zhang Y, Zhang Y (2017) Novel nanostructured MIL-101(Cr)/XC-72 modified electrode sensor: a highly sensitive and selective determination of chloramphenicol. Sens Actuators B 247:756–764
12. Zhao X, Zhang Q, Chen H, Liu G, Bai W (2017) Highly sensitive molecularly imprinted sensor based on platinum thin-film microelectrode for detection of chloramphenicol in food samples. Electroanalysis 29:1918–1924
13. Kong F-Y, Chen T-T, Wang J-Y, Fang H-L, Fan DH, Wang W (2016) UV-assisted synthesis of tetrapods-like titanium nitride-reduced graphene oxide nanohybrids for electrochemical determination of chloramphenicol. Sens Actuators B 225:298–304
14. Yan Z-D, Gan N, Li T-H, Cao Y-T, Chen Y-J (2016) A sensitive electrochemical aptasensor for multiplex antibiotics detection based on high-capacity magnetic hollow porous nanotracers coupling exonuclease-assisted cascade target recycling. Biosens Bioelectron 78:51–57
15. Sun Y, Wei T, Jiang M, Xu L, Xu Z (2018) Voltammetric sensor for chloramphenicol determination based on a dual signal enhancement strategy with ordered mesoporous carbon@polydopamine and β-cyclodextrin. Sens Actuators B 255:2155–2162
16. Yang R-R, Zhao J-L, Chen M-J, Yang T, Luo S-Z, Jiao K (2015) Electrocatalytic determination of chloramphenicol based on molybdenum disulfide nanosheets and self-doped polyaniline. Talanta 131:619–623
17. Sakthivel M, Sukanya R, Chen S-M, Ho K-C (2018) Synthesis and characterization of samarium-substituted molybdenum diselenide and its graphene oxide nanohybrid for enhancing the selective sensing of chloramphenicol in a milk sample. ACS Appl Mater Interfaces 10:29712–29723
18. Socas-Rodríguez B, González-Sálamo J, Hernández-Borges J, Rodríguez-Delgado MA (2017) Recent applications of nanomaterials in food safety. Trend Anal Chem 96:172–200
19. Wu D, Du D, Lin Y (2016) Recent progress on nanomaterial-based biosensors for veterinary drug residues in animal-derived food. Trend Anal Chem 83:95–101
20. Zhu C, Yang G, Li H, Du D, Lin Y (2015) Electrochemical sensors and biosensors based on nanomaterials and nanostructures. Anal Chem 87:230–249
21. Yalikun N, Mamat X, Li Y, Hu X, Wågberg T, Dong Y, Hu G (2018) Synthesis of an iron-nitrogen co-doped ordered mesoporous carbon-silicon nanocomposite as an enhanced electrochemical sensor for sensitive and selective determination of chloramphenicol. Colloid Surf B 172:98–104
22. Cheng C, Li S, Thomas A, Kotov NA, Haag R (2017) Functional graphene nanomaterials based architectures: biointeractions, fabrications, and emerging biological applications. Chem Rev 117:1826–1914
23. Borowiec J, Wang R, Zhu L, Zhang J (2013) Synthesis of nitrogen-doped graphene nanosheets decorated with gold nanoparticles as an improved sensor for electrochemical determination of chloramphenicol. Electrochim Acta 99:138–144
24. Zhai H, Liang Z, Chen Z, Wang H, Liu Z, Su Z, Zhou Q (2015) Simultaneous detection of metronidazole and chloramphenicol by differential pulse stripping voltammetry using a silver nanoparticles/sulfonate functionalized graphene modified glassy carbon electrode. Electrochim Acta 171:105–113
25. Liu S, Lai G, Zhang H, Yu A (2017) Amperometric aptasensing of chloramphenicol at a glassy carbon electrode modified with a nanocomposite consisting of graphene and silver nanoparticles. Microchim Acta 184:1445–1451
26. Pumera M (2014) Heteroatom modified graphenes: electronic and electrochemical applications. J Mater Chem C 2:6454–6461
27. Chen N, Huang X, Qu L (2015) Heteroatom substituted and decorated graphene: preparation and applications. Phys Chem Chem Phys 17:32077–32098

28. Paraknowitsch JP, Thomas A (2013) Doping carbons beyond nitrogen: an overview of advanced heteroatom doped carbons with boron, sulphur and phosphorus for energy applications. Energy Environ Sci 6:2839–2855
29. Choi CH, Park SH, Woo SI (2012) Binary and ternary doping of nitrogen, boron, and phosphorus into carbon for enhancing electrochemical oxygen reduction activity. ACS Nano 6:7084–7091
30. Zhang X, Wang K-P, Zhang L-N, Zhang Y-C, Shen L (2018) Phosphorus-doped graphene-based electrochemical sensor for sensitive detection of acetaminophen. Anal Chim Acta 1036:26–32
31. Cote LJ, Kim F, Huang J (2009) Langmuir-Blodgett assembly of graphite oxide single layers. J Am Chem Soc 131:1043–1049
32. Zhang X, Zhang B, Liu D-Y, Qiao J-L (2015) One-pot synthesis of ternary alloy CuFePt nanoparticles anchored on reduced graphene oxide and their enhanced electrocatalytic activity for both methanol and formic acid oxidation reactions. Electrochim Acta 177:93–99
33. Zhang X, Zhang Y-C, Ma L-X (2016) One-pot facile fabrication of graphene-zinc oxide composite and its enhanced sensitivity for simultaneous electrochemical detection of ascorbic acid, dopamine and uric acid. Sens Actuators B 227:488–496
34. Bard AJ, Faulkner LR (2001) Electrochemical methods: fundamentals applications, 2nd edn. Wiley, New York
35. Chen X, Wang Y, Zhou J, Yan W, Li X, Zhu JJ (2008) Electrochemical impedance immunosensor based on three-dimensionally ordered macroporous gold film. Anal Chem 80:2133–2140
36. Pei S, Cheng H-M (2012) The reduction of graphene oxide. Carbon 50:3210–3228
37. Dettlaff-Weglikowska U, Skákalová V, Graupner R, Jhang SH, Kim BH, Lee HJ, Ley L, Park YW, Berber S, Tománek D, Roth S (2005) Effect of $SOCl_2$ treatment on electrical and mechanical properties of single-wall carbon nanotubes networks. J Am Chem Soc 127:5125–5131
38. Codognoto L, Winter E, Doretto KM, Monteiro GB, Rath S (2010) Electroanalytical performance of self-assembled monolayer gold electrode for chloramphenicol determination. Microchim Acta 169:345–351
39. Munawar A, Tahir MA, Shaheen A, Lieberzeit PA, Khan WS, Bajwa SZ (2018) Investigating nanohybrid material based on 3D CNTs@Cu nanoparticle composite and imprinted polymer for highly selective detection of chloramphenicol. J Hazard Mater 342:96–106